

First-principles calculations of F-, Cl-, and N-related defects of amorphous SiO_2 and their impacts on carrier trapping and proton release

Xin Gao(高鑫), Yunliang Yue(乐云亮), Yang Liu(刘杨), and Xu Zuo(左旭)†
Citation: Chin. Phys. B, 2021, 30 (**4**): 047104. DOI: 10.1088/1674-1056/abe3f7
Journal homepage: http://cpb.iphy.ac.cn; http://iopscience.iop.org/cpb

What follows is a list of articles you may be interested in

Ultra-low Young's modulus and high super-exchange interactions in monolayer CrN: A promising candidate for flexible spintronic applications

Yang Song(宋洋), Yan-Fang Zhang(张艳芳), Jinbo Pan(潘金波), and Shixuan Du(杜世萱)
Chin. Phys. B, 2021, 30 (**4**): 047105. DOI: 10.1088/1674-1056/abdb20

Passivation of PEA^+ to $MAPbI_3$ (110) surface states by first-principles calculations

Wei Hu(胡伟), Ying Tian(田颖), Hong-Tao Xue(薛红涛), Wen-Sheng Li(李文生), and Fu-Ling Tang(汤富领)
Chin. Phys. B, 2021, 30 (**4**): 047101. DOI: 10.1088/1674-1056/abccb7

Structure prediction, electronic, and mechanical properties of alkali metal MB_{12} (*M*= *Be*, Mg, Ca, Sr) from first principles

Chun-Ying Pu(濮春英), Rong-Mei Yu(于荣梅), Ting Wang(王婷), Zhen-Yan X\"ue(薛振彦), Yong-Sheng Zhu(朱永胜), and Da-Wei Zhou(周大伟)
Chin. Phys. B, 2021, 30 (**1**): 017102. DOI: 10.1088/1674-1056/abb667

Two-dimensional hexagonal Zn_3Si_2 monolayer: Dirac cone material and Dirac half-metallic manipulation

Yurou Guan(官雨柔), Lingling Song(宋玲玲), Hui Zhao(赵慧), Renjun Du(杜仁君), Liming Liu(刘力铭), Cuixia Yan(闫翠霞), Jinming Cai(蔡金明)
Chin. Phys. B, 2020, 29 (**8**): 087103. DOI: 10.1088/1674-1056/ab943a

Electronic structures, magnetic properties, and martensitic transformation in all-d-metal Heusler-like alloys Cd_2MnTM(*TM*=Fe, Ni, Cu)

Yong Li(李勇), Peng Xu(徐鹏), Xiaoming Zhang(张小明), Guodong Liu(刘国栋), Enke Liu(刘恩克), Lingwei Li(李领伟)
Chin. Phys. B, 2020, 29 (**8**): 087101. DOI: 10.1088/1674-1056/ab9739

First-principles calculations of F-, Cl-, and N-related defects of amorphous SiO_2 and their impacts on carrier trapping and proton release*

Xin Gao(高鑫)[1], Yunliang Yue(乐云亮)[2], Yang Liu(刘杨)[3,4], and Xu Zuo(左旭)[1,5,6,†]

[1] College of Electronic Information and Optical Engineering, Nankai University, Tianjin 300071, China
[2] School of Information Engineering, Yangzhou University, Yangzhou 225127, China
[3] Microsystem and Terahertz Research Center, China Academy of Engineering Physics, Chengdu 610200, China
[4] Institute of Electronic Engineering, China Academy of Engineering Physics, Mianyang 621999, China
[5] Municipal Key Laboratory of Photo-electronic Thin Film Devices and Technology, Nankai University, Tianjin 300071, China
[6] Engineering Research Center of Thin Film Optoelectronics Technology, Ministry of Education, Tianjin 300071, China

(Received 30 December 2020; revised manuscript received 3 February 2021; accepted manuscript online 8 February 2021)

The first-principles calculations based on density functional theory are performed to study F-, Cl-, and N-related defects of amorphous SiO_2 (a-SiO_2) and their impacts on carrier trapping and proton release. The possible geometric configurations of the impurity-related defects, the formation energies, the hole or electron trapping of the neutral defects, and the mechanisms to suppress proton diffusion by doping N are investigated. It is demonstrated by the calculations that the impurity atoms can interact with the oxygen vacancies and result in impurity-related defects. The reactions can be utilized to saturate oxygen vacancies that will cause ionization damage to the semiconducting devices. Moreover, the calculated formation energy indicates that the F- or Cl-related oxygen vacancy defect is a deep hole trap, which can trap holes and prevent them from diffusing to the a-SiO_2/Si interface. However, three N-related defects, namely N(2)o–H, N(2)o=O, and N(3)o–V_o, tend to act as shallow hole traps to facilitate hole transportation during device operation. The N(2)o and N(3)o configurations can be negatively charged as deep electron traps during the oxide charge buildup after ionization radiation. In addition, the nudged elastic band (NEB) calculations show that four N-related defects, namely N(2)o, N(2)o–H, N(2)o=O, and N(3)o are capable of capturing protons and preventing them from diffusing to and de-passivating the interface. This research reveals the fundamental properties of the F-, Cl-, and N-related defects in amorphous silica and the details of the reactions of the carrier trapping and proton release. The findings help to understand the microscopic mechanisms that alleviate ionization damage of semiconducting devices by doping a-SiO_2.

Keywords: first-principles calculation, doping, defect, proton

PACS: 71.15.Mb, 71.20.–b, 61.72.Bb, 61.80.Az **DOI:** 10.1088/1674-1056/abe3f7

1. Introduction

SiO_2/Si interface plays an important role in semiconductor devices and has a great influence on device reliability. Ionization radiation can induce electron-hole pairs in SiO_2, which will drift under the gate electric field. The holes will migrate to the interface transition area and activate the interface defects.[1] Protons will also activate the hydrogenated defects and degrade the interface performance. These reactions ultimately lead to ionization damage at the a-SiO_2/Si interface that causes device degeneration or even failure.[2–5]

In this paper, the first-principles calculations based on density functional theory are performed to study F-, Cl-, and N-related defects of a-SiO_2 and their impacts on proton release. There are two main processes for generating protons. First, hydrogenation defects and protons (H^+) will form if hydrogen molecules break at positively charged oxygen vacancy defects.[6,7] Second, the H-containing defects could also release protons by hole capture under the irradiation condition.[7,8] Previous studies have also shown that the suspension bond of oxygen vacancy can be terminated by doping of Cl to reduce oxygen vacancy and improve the reliability of a-SiO_2.[9] In this work, we have investigated the possible configurations formed by the interaction of F, Cl, and oxygen vacancy defects. After the conversion of the oxygen vacancy defects to F/Cl related structures, the concentration of oxygen vacancies is reduced, and the reaction of molecular hydrogen and positively charged oxygen vacancy defects is suppressed. The newly formed defects are found to be effective deep traps, which reduce the amount of the holes that can be trapped by the hydrogen-containing defects. Both effects suppress the proton release process.

Due to the anti-radiation properties of N-containing SiO_2,[10,11] Jeong *et al.* constructed several N-containing defect models and suggested that the coexistence of N and H

*Project supported by the Science Challenge Project (Grant No. TZ2016003-1-105), CAEP Microsystem and THz Science and Technology Foundation (Grant No. CAEPMT201501), the National Basic Research Program of China (Grant No. 2011CB606405), and Tianjin Natural Science Foundation, China (Grant No. 20JCZDJC00750).

†Corresponding author. E-mail: xzuo@nankai.edu.cn

© 2021 Chinese Physical Society and IOP Publishing Ltd

improves the electrical reliabilities of Si oxynitride films.[12] Orellana *et al.* studied NO, NH, N_2, and atomic N interacting with a Si-Si bond of an otherwise perfect SiO_2.[13] In this paper, we discuss the neutral defect configuration of N in the a-SiO_2 model, positively charged structures formed after neutral defects trap holes, and the formation energy of these structures. N-containing defects will compete with oxygen vacancies defects or hydrogenated defects to reduce the latter's probability of trapping holes. Further, the N-containing defects are found to be proton traps, which prevent protons from spreading to the interface.

2. Methods

Under the theoretical framework of density functional theory (DFT), the Perdew–Burke–Ernzerhof (PBE) parameterization of general gradient approximation (GGA) is used to perform the first-principles calculation in the Vienna *ab initio* simulation package (VASP) software. The role of the valence electron and the real part of the atom is described by the projected augmented-wave method. The cut-off energy of plane wave expansion is set to 520 eV. Brillouin-zone integration is performed on the Γ point due to the large size of the unit cell. The convergence criterion for structural optimization is that the total energy difference is lower than 10^{-4} eV, and the criterion for electronic self-consistent iteration is raised to 10^{-5} eV. The defect-free a-SiO_2 model is taken from Ref. [14], where 216 atoms in a periodic unit are considered and the dimension of the supercells in this work is about $16.5\times16.5\times12.4$ Å^3.

To determine the relative stability and electrical properties of the impurity-forming structure, the formation energy and transition energy levels of various defect structures in the neutral and positively charged states are calculated under the O-rich and Si-rich conditions. The bandgap of a-SiO_2 is underestimated by GGA. To relieve the problem, we apply the unscreened hybrid functional in which 35% of PBE exchange is replaced by the Hartree–Fock exchange. In the present work, the formula of formation energy is referred to as the formalism defined by Van de Walle *et al.*[15]

$$E^{\mathrm{f}}[X^q] = E_{\mathrm{tot}}[X^q] - E_{\mathrm{tot}}[\mathrm{bulk}] - \sum_i n_i u_i + qE_{\mathrm{F}} + E_{\mathrm{corr}}, \quad (1)$$

where $E_{\mathrm{tot}}[X^q]$ is the total energy of a-SiO_2 model containing defect X with charge q, and $E_{\mathrm{tot}}[\mathrm{bulk}]$ is the total energy of the same bulk a-SiO_2 model, $n_i u_i$ is the chemical potential for adding or subtracting atoms. At the O-rich condition (oxidizing condition), $\mu_{\mathrm{O}} = 1/2\mu_{\mathrm{O_2}}$. E_{corr} is the correction term due to system electrification. In this work, the energy of the state of charge is corrected by calculating the change in electrostatic potential from the period to the open boundary condition. E_{corr} is the correction for charged systems proposed by Freysoldt, Neugebauer, and Van de Walle.[16]

3. Results and discussions

3.1. The configurations of atomic F/Cl decorated oxygen vacancies and N related defects

To simulate the interaction between atomic F, Cl, and oxygen vacancies in a-SiO_2, the central oxygen atom bonding with Si atoms is removed, and all systems are relaxed to make O vacancy in defect-free a-SiO_2. Ten neutral dimer configurations are obtained. The length of the Si-Si dimer is 2.43 Å on average, similar to the values in the previous report.[17]

An atomic F is added in the a-SiO_2 model surrounding the vacancy as the starting structure. After relaxation, the structure shown in Fig. 1 is obtained. The F atom is connected to one of the Si atoms, and the other Si atom carries an unpaired electron. The length between two Si atoms increases to 3.31 Å, and the average Si–F length is 1.62 Å. The interaction structure of the Cl atom and the oxygen vacancy is the same as that of the F atom, and the only difference is the bond length. For the Cl passivated defect, the length between two Si atoms increases to 3.06 Å, and the average Si–Cl length is 2.12 Å, which is 0.5 Å longer than the Si–F length.

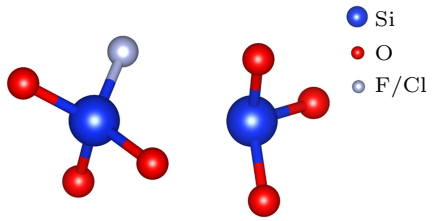


Fig. 1. Defect configuration generated by the interaction of an F or Cl atom and an oxygen vacancy.

It has been reported that the coexistence of N and H can effectively eliminate the hole trap.[18] During the proton release process, N-doped a-SiO_2 may react with both holes and protons, thereby influencing the proton release process. Therefore, possible configurations of N-related defects in a-SiO_2 were investigated (Fig. 2). Substituting an N atom for an O atom in the defect-free silica network, connecting two Si atoms and performing structural relaxation, the N(2)o structure is obtained (Fig. 2(b)). The length of Si–N is 1.71 Å on average. This article adopts the same structure naming method as in Ref. [19]. The symbol N represents N atom, the number represents the N atom coordination number, and the lowercase O represents N atom instead of O atom. In the N(2)o=O structure (Fig. 2(c)), an O atom is added to the N(2)o structure and an N–O bond is formed; the average Si–N bond length is about 1.78 Å. The structure of N(2)o–H is similar to N(2)o=O, an H atom is added to the N(2)o structure and an N–H bond is formed (Fig. 2(d)), the Si–N bond length does not change much compared to that of N(2)o. The average value is about 1.72 Å. Based on the N(2)o structure, the N atom is connected with another Si atom to form a threefold N atom, the N(3)o structure is obtained (Fig. 2(f)); the connecting oxygen atom

of this silicon atom is removed to form a new structure named N(3)o–V_o as shown in Fig. 2(e). The Si–N bond length is increased by 0.05 Å compared to the N(2)o structure, reaching an average value of 1.76 Å, and the bond angle of the threefold N atom is between 116° and 120°. In the meantime, the N atom and the three Si atoms connected are almost in the same plane. The bond length and bond angle of these structures are very similar to those previously reported in α-quartz.[12] All structures have been observed in experiments.[20–23] N(2)o and N(3)o are the two structures that occur most frequently.[20]

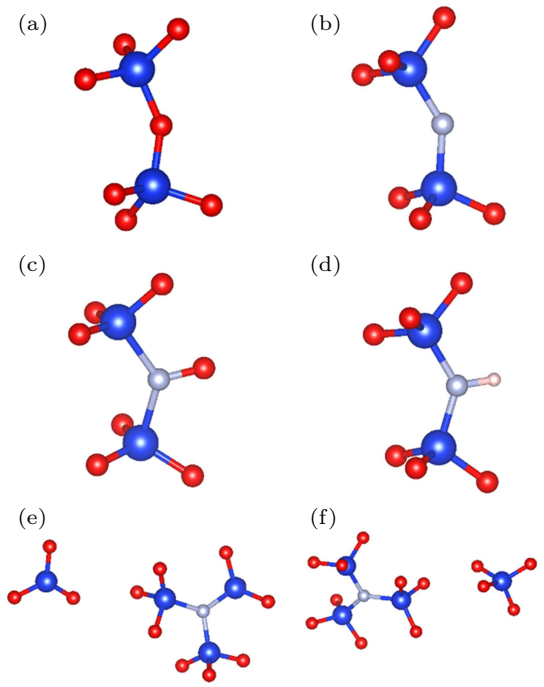


Fig. 2. Possible configurations of N-related defects in a-SiO_2 (a) defect-free a-SiO_2, (b) N(2)o, (c) N(2)o=O, (d) N(2)o–H, (e) N(3)o–V_o, (f) N(3)o.

3.2. Hole trapping at the neutral defect centers

Hole trapping at a-SiO_2 doped defects was simulated by removing an electron from the unit cell and then optimized the structure. F- and Cl-defects of a-SiO_2 converge into two different structures via hole trapping (Fig. 3). First, the atomic F or Cl is connected between two Si atoms to form a Si–F–Si/Si–Cl–Si bridge configuration (Fig. 3(a)). Alternatively, the doping atoms are connected to the one Si atom, and the other is in an sp^2 state at a threefold coordinated silicon atom (Fig. 3(b)). In this configuration, the Si–O bond decreases to an average value of 1.57 Å compared to the neutral charge state and the four atoms are almost in the same plane.

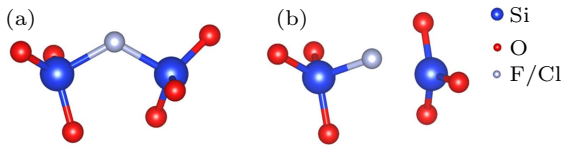


Fig. 3. Positively charged F- and Cl-related defect configuration (a) Si–F/Cl–Si bridge configuration, (b) sp^2 Si configuration.

As for N-related defects, all of them still maintain the original configuration, but the bond length and the bond angle have changed with respect to the neutral structure. In the positively charged N(2)o configuration shown in Fig. 4(a), the Si–Si distance increases to 3.46 Å on average and the Si–N distance increases to about 1.78 Å compared to the neutral charge state. The total magnetic moment increases from 1.0 μ_B to 2.0 μ_B, and the spin density mainly resides on the nitrogen atom. Some of them spread over the two connected silicon atoms and the three coordination oxygen atoms adjacent to the silicon atoms. In the positively charged N(2)o=O (Fig. 4(b)), the Si–N bonds (bond lengths ∼ 1.95 Å) are longer than the Si–N bonds (average bond length ∼ 1.78 Å) in the neutral structure and the Si–N–Si bond angle increases from 105° to 112°. The positively charged structure is closer to a planar structure than a neutral structure. The total magnetic moment decreases from 1.0 μ_B to 0 μ_B. The spin densities in the neutral structure show that the unpaired electron spins are mainly located on p orbitals of the nitrogen and oxygen atoms. In the positively charged N(2)o–H configurations shown in Fig. 4(c), the average Si–Si distance increases to 3.28 Å and the Si–N distance increases to about 1.78 Å compared to the neutral charge state.

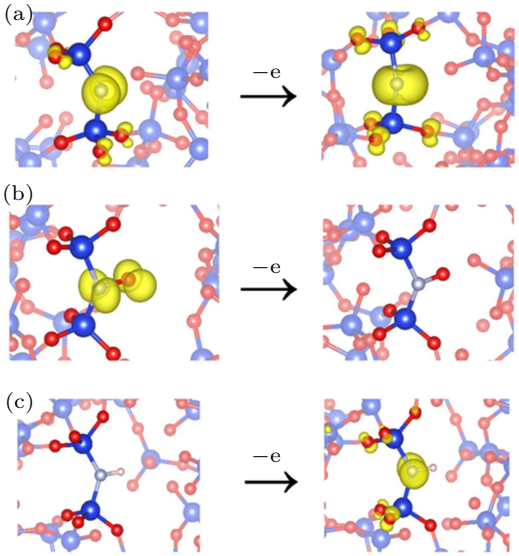


Fig. 4. Positively charged N-related defect configurations (a) N(2)o, (b) N(2)o=O, (c) N(2)o–H.

The spin density is mostly localized at the silicon dangling bond in the neutral N(3)o–V_o configurations, and the three coordination silicon atom is in the sp^2 state after capturing the hole, as shown in Fig. 5(a). When the neutral structure in Fig. 5(b) captures hole, unlike in Fig. 5(a), the spin-charge density is localized on the three-coordinated N atom instead of being captured by the oxygen atom connected to the Si atom. The spin density mainly resides on the nitrogen and oxygen atoms, and the total magnetic moment changed from 1 μ_B to 2 μ_B.

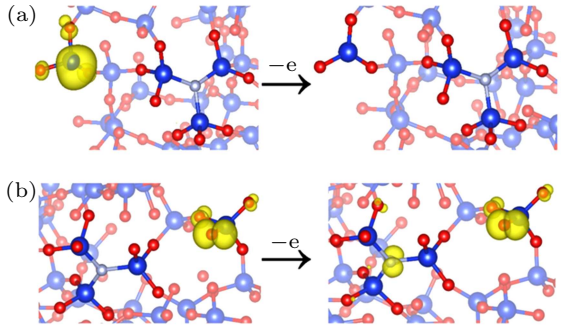


Fig. 5. Positively charged N-related defect configurations. (a) N(3)o-V_o, (b) N(3)o.

3.3. Formation energy

Based on the above research, the formation energies of neutral and ±1 charged F-, Cl-, and N-related defects were calculated. The results are shown in Fig. 6. The slope of the straight line indicates the charged state, and the sloping-up, horizontal, and slopping down segments are associated with the +1, 0, and −1 charge states, respectively. The meter level is aligned with the top of the valence band of a-SiO_2 without defects, and the shaded area indicates the bandgap of Si. The transition levels of different structures can be obtained from Fig. 6.

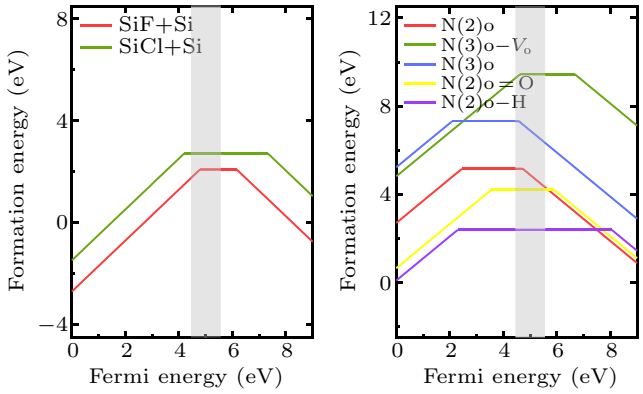


Fig. 6. Formation energy as a function of Fermi energy for the F-, Cl-, and N-related defect. The sloping-up, horizontal, and slopping down segments are associated with the +1, 0, and −1 charge states, respectively.

The results show that the Cl formation energy is the highest when the system is uncharged. And the energy levels suggest the defects are deep energy traps that prevent the holes from diffusing to the interface.

The Fermi energy lies approximately in the middle of silicon bandgap for most devices. For several structures obtained by N doping, N(2)o–H has the lowest formation energy while the Fermi level in the silicon bandgap. In contrast, N(3) structure has the highest formation energy. N(2)o–H, N(2)o=O, and N(3)o–V_o during device operation exist in a neutral state and act as shallow traps to transport holes. The N(2)o and N(3)o configurations, whose transition levels from neutral to negatively charged states are in the silicon bandgap, could be negatively charged as the deep electron traps during the oxide charge buildup after ionization radiation.

3.4. Proton traps

N-containing defects will become proton traps to prevent protons from spreading to the interface due to the coordination number of N. To simulate the reaction of a proton with an N-containing defect, an H atom is placed near the gap, and an electron is subtracted from the system to simulate a proton. According to the Bader charge analysis, the numbers of valence electrons on H atoms are zero in all four of these structures. The structures are shown in Fig. 7.

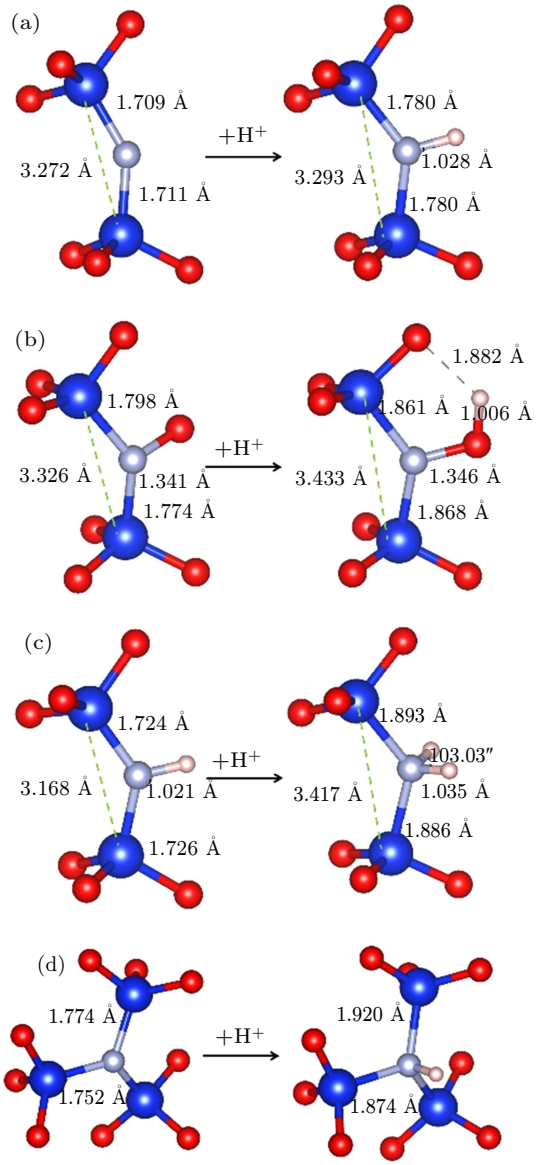


Fig. 7. Proton captured by the N-related defects. (a) N(2)o, (b) N(2)o=O, (c) N(2)o–H, (d) N(3)o.

In the N(2)o configuration shown in Fig. 7(a), a proton attaches to the atomic N and the average Si–N distance increases to 1.78 Å. In the N(2)o=O configuration, the proton attaches to the oxygen bonded to the atomic N. The Si–N bonds (bond lengths ∼ 1.86 Å) are longer than the Si–N bonds (average bond length ∼ 1.78 Å) in the structure without proton and the Si–N-Si bond angle increases from 105° to 112°. The latter configuration is closer to a planar structure than the former.

For the N(2)o–H configuration, the proton attaches to atomic N and the Si–N bonds increase to 1.89 Å on average. For the N(3)o configuration, the Si–N bonds (bond lengths ∼ 1.89 Å) are longer than the Si–N bonds (average bond length ∼ 1.76 Å) in the structure without proton.

Previous studies have calculated the energies of the three coordination N configurations in SiO_2 before and after the trap of protons. It has been claimed that nitrogen can be an effective trapping center for hydrogen ions.[24] However, the paper only considered the capability to capture protons by the tricoordination N defect but did not consider that whether the trapped hydrogen ions can continue to diffuse along with the oxygen atoms or not. Protons usually jump and diffuse between adjacent oxygen atoms in silica.[25] Depassivation occurs when protons diffuse to the interface, which will degrade the interface performance.[26,27] For the N(2)o structure, the diffusion process of hydrogen ions from N-containing defects to oxygen atoms is simulated by the nudged elastic band calculation, which gives the reaction curve connecting the initial and final states and the transition state associated with the energy barrier (Fig. 8). The reaction starts from the initial state where the proton is attached to an N atom. The energy of the reaction curve increases and reaches the maximum in the transition state when the proton moves to the adjacent oxygen atom. In the final state, the proton is connected to the O atom. The energy is 1.25 eV higher than the initial state, so the reaction is endothermic. The reaction from the initial state to the final state is more difficult; hence protons (H^+) tend to attach to the nitrogen bridges in a-SiO_2.

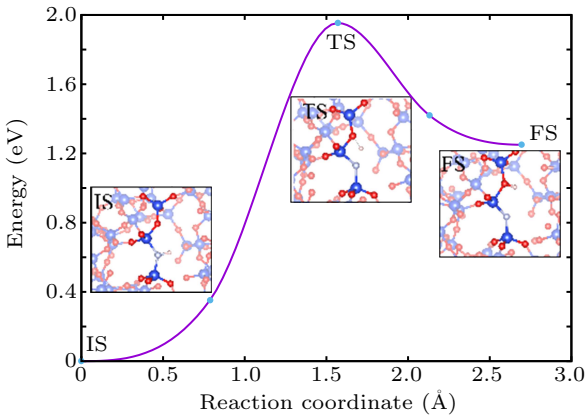


Fig. 8. The reaction curve of the detrap of the proton captured by the N(2)o configuration. The initial, transition, and final structures are illustrated in the insets.

For the N(2)o–H structure, the diffusion process of a proton from N(2)o–H to oxygen atoms is also investigated, and the reaction curve is plotted in Fig. 9. In the final state, the energy is 1.71 eV higher than the initial state. We can draw the same conclusion as N(2)o, that is N(2)o–H defects are easier to capture protons and it is difficult for the captured protons to diffuse along with the oxygen.

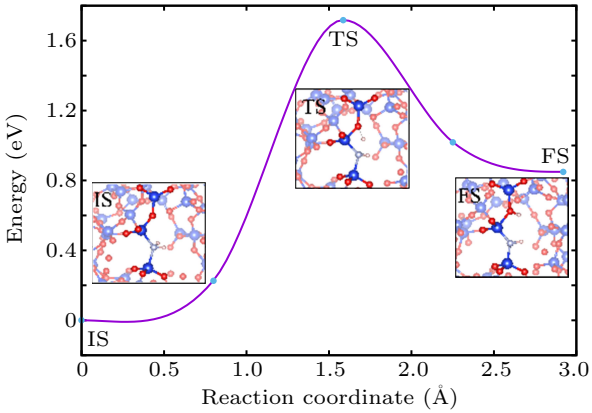


Fig. 9. The reaction curve of the detrap of the proton in N(2)o–H structure. The initial, transition, and final structures are illustrated in the insets.

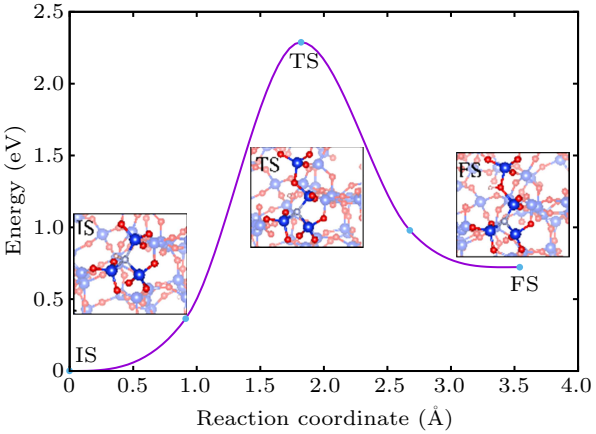


Fig. 10. The reaction curve of the detrap of the proton captured by N(3)o structure. The initial, transition, and final structures are illustrated in the insets.

For the N(3)o structure, the diffusion process of the proton is plotted in Fig. 10. The reaction starts from the initial state where the proton is attached to a threefold N atom. When the proton moves to the adjacent oxygen atom, the positive reaction barrier is as high as 2.28 eV, and it is almost impossible to dissociate. In the final state, the energy is 0.72 eV higher than the initial state, so the reaction is also endothermic and protons tend to attach to nitrogen; thus, the defect center of tricoordinate N is more comfortable to capture proton.

The diffusion of protons from the N(2)o=O structure to the oxygen atom has also been studied. However, in the NEB calculation process, the final state of the proton connected to the adjacent oxygen atom cannot be obtained because the oxygen atom connected to the N atom in the initial structure is easy to capture protons. In summary, N-containing defects are easier to capture protons, and it is challenging for the captured protons to diffuse along with the oxygen. Thus N-containing defects can prevent the occurrence of interface depassivation reaction.

4. Conclusion

The F-, Cl-, and N-related defects in a-SiO_2 are studied by the first-principles calculations based on density functional

theory. The defects are obtained by interacting an F or Cl atom with an oxygen vacancy or by optimizing the N-related defects constructed in the defect-free models. The structure relation and the formation energies of the F-, Cl-, and N-related defects after trapping a hole are investigated. The results suggest that F and Cl atoms can passivate oxygen vacancy defects. The resulting defects induce the charge transition levels deep in the bandgap, which can trap holes and then suppress their diffusion. In a practical transistor, if the silicon base attached to the a-SiO_2 is not highly p-doped, the two configurations of N-related defects (N(2)o and N(3)o) are negative charge traps which can also compensate the excess holes excited by the irradiations. The capability of the N-related defects to capture protons is also investigated. It is shown by the calculations that the N-related defects can trap protons hence can serve as proton sink to suppress proton diffusion and the following depassivation of a-SiO_2/Si interface. This work pushes forward the research of the impurity-related defects in a-SiO_2 by providing the fundamental parameters of the structure, formation energy, charge transition level, and proton capture reaction. These findings contribute to understanding the impacts of impurities on the ionization damage of semiconducting devices and pave a way to alleviate the damage by rationally doping of a-SiO_2.

References

[1] Schwank J R, Shaneyfelt M R, Fleetwood D, *et al.* 2008 *IEEE Trans Nucl Sci.* **55** 1833
[2] Bongiorno A and Pasquarello A 2004 *Phys. Rev. B* **70** 195312
[3] Deal B E and Grove A S 1965 *J. Appl. Phys.* **36** 3770
[4] Ganster P, Tréglia G and Saúl A 2010 *Phys. Rev. B.* **81** 045315
[5] Huang S P, Zhang R Q, Li H S, *et al.* 2009 *J. Phys. Chem. C* **113** 12736
[6] Tuttle B R, Hughart D R, Schrimpf R D, Fleetwood D M and Pantelides S T 2010 *IEEE Trans. Nucl. Sci.* **57** 3046
[7] Yue Y, Song Y and Zuo X 2018 *Chin. Phys. B.* **27** 037102
[8] Rowsey N L, Law M E, Schrimpf R D, *et al* 2011 *IEEE Trans. Nucl. Sci.* **58** 2937
[9] Yokozawa A and Miyamoto Y 1998 *Appl. Phys. Lett.* **73** 1122
[10] Tan S S, Chen T P, Soon J M, Loh K P, Ang C H, Teo W Y and Chan L 2003 *Appl. Phys. Lett.* **83** 530
[11] Schmidt P F, Rand M J, Mitchell J P and Ashner J D 1969 *IEEE Trans. Nucl. Sci.* **16** 211
[12] Jeong S and Oshiyama A 2001 *Phys. Rev. Lett.* **86** 3574
[13] Orellana W, da Silva A J R and Fazzio A 2004 *Phys. Rev. B* **70** 125206
[14] El-Sayed A M, Watkins M B, Afanas'ev V V, *et al* 2014 *Phys. Rev. B* **89** 125201
[15] Van de Walle and C G Neugebauer J 2004 *J. Appl. Phys.* **95** 3851
[16] Freysoldt C, Neugebauer J and Walle C G V D 2009 *Phys. Rev. Lett.* **102** 016402
[17] Tamura T, Lu G H, Yamamoto R, *et al*. 2004 *Phys. Rev. B* **69** 195204
[18] Jeong S and Oshiyama A 2001 *Physica B* **308** 999
[19] Lee E C and Chang K J 2002 *Phys. Rev. B* **66** 233205
[20] Ono H, Ikarashi T, Miura Y, Hasegawa E, Ando K, Kitano T 1999 *Appl. Phys. Lett.* **74** 203
[21] Bhat M, Yoon G W, Kim J, Kwong D L, Arendt M and White J M 1994 *Appl. Phys. Lett.* **64** 2116
[22] Hegde R I, Tobin P J, Reid K G, Maiti B and Ajuria S A 1995 *Appl. Phys. Lett.* **66** 2882
[23] Carr E C and Buhrman R A 1993 *Appl. Phys. Lett.* **63** 54
[24] Tan S S, Chen T P, Soon J M, Loh K P, Ang C H, Teo W Y and Chan L 2003 *Appl. Phys. Lett.* **83** 530
[25] Godet J and Pasquarello A 2006 *Phys. Rev. Lett.* **97** 155901
[26] Rasnkeev S N, Fleetwood D M, SchrimpfF R D, *et al*. 2004 *IEEE Trans. Nucl. Sci.* **51** 3158
[27] Chen X J, Barnaby H J, VermeireERME B, *et al*. 2007 *IEEE Trans. Nucl. Sci.* **54** 1913